Article

Thermally-Induced Structural Transitions between Single-Crystalline States in the First Hybrid Compound Combining Keggin-Type Clusters with Metal-Cyclam Complexes: From 2-Dimensional Covalent Assemblies to Discrete Molecular Species

Leticia Fernández-Navarro, Amaia Iturrospe, Santiago Reinoso, Beñat Artetxe, Estibaliz Ruiz-Bilbao, Leire San Felices, and Juan M. Gutierrez-Zorrilla

Cryst. Growth Des., **Just Accepted Manuscript** • DOI: 10.1021/acs.cgd.0c00286 • Publication Date (Web): 01 Apr 2020

Thermally-Induced Structural Transitions between Single-Crystalline States in the First Hybrid Compound Combining Keggin-Type Clusters with Metal-Cyclam Complexes: From 2-Dimensional Covalent Assemblies to Discrete Molecular Species

Leticia Fernández-Navarro,[‡] Amaia Iturrospe,[⊥] Santiago Reinoso,[§] Beñat Artetxe,[*,‡] Estibaliz Ruiz-Bilbao,[‡] Leire San Felices,[∥] and Juan M. Gutiérrez–Zorrilla[*,†,‡]

[‡]Departamento de Química Inorgánica, Facultad de Ciencia y Tecnología, Universidad del País Vasco UPV/EHU, P.O. Box 644, 48080 Bilbao, Spain.

[⊥]Centro de Física de Materiales CFM (CSIC–UPV/EHU), Paseo Manuel Lardizábal 5, 20018 Donostia-San Sebastián, Spain

[§]Departamento de Ciencias, and Institute for Advanced Materials and Mathematics (InaMat²), Universidad Pública de Navarra (UPNA), Campus de Arrosadia, 31006 Pamplona, Spain.

[∥]Servicios Generales de Investigación SGIker, Facultad de Ciencia y Tecnología, Universidad del País Vasco UPV/EHU, P.O. Box 644, 48080 Bilbao, Spain.

[†]BCMaterials, Basque Center for Materials, Applications and Nanostructures, UPV/EHU Science Park, 48940 Leioa, Spain.

ABSTRACT: Hydrothermal reaction between the monolacunary polyoxometalate $[SiW_{11}O_{39}]^{8-}$, a copper(II) salt and 1,4,8,11-tetraazacyclotetradecane (cyclam) affords the first example of a hybrid compound combining metal complexes of such N4-tetradentate macrocyclic ligand and Keggin-type clusters, namely $[Cu(cyclam)(H_2O)][\{Cu(cyclam)\}_2SiW_{11}O_{39}Cu(H_2O)]\cdot 5H_2O$ (**1**). This compound has been characterized by infrared spectroscopy, thermal and elemental analyses. Single-crystal X-ray diffraction (scXRD) reveals a layered crystal packing made of corrugated 2-dimensional covalent grids in which four octahedral $\{Cu(cyclam)\}^{2+}$ bridging moieties connect copper(II)-monosubstituted $\{SiW_{11}O_{39}Cu(H_2O)\}^{6-}$ polyanions to four adjacent clusters, and additional $[Cu(cyclam)(H_2O)]^{2+}$ square-pyramidal counterions are embedded into square-like grid voids. Thermo-structural analyses confirms the presence in the 130–250 °C temperature range of a stable and crystalline anhydrous phase, which displays a diffraction pattern different from that of **1**. This thermally-triggered phase transition proceeds through a single-crystal to single-crystal transformation pathway, which according to scXRD, involves not only the release of water molecules, but also the cleavage and formation of Cu–O bonds induced by the rotation of Keggin-type anions. These modifications fully dismantle the parent 2-dimensional covalent assembly to result in the neutral, discrete $[\{Cu(cyclam)\}_3SiW_{11}O_{39}Cu]$ hybrid species (**2**), in which the cluster exhibits three square-pyramidal $\{Cu(cyclam)\}^{2+}$ decorating moieties grafted at its surface. This species must display a 5-coordinated copper(II) center in the Keggin skeleton, and therefore, it constitutes one of the scarce examples of such type of coordinatively unsaturated substituted cluster observed in the solid state. The irreversibility of the phase transition has been confirmed by combined thermal and diffractometric analyses, which evidenced also the great flexibility of the supramolecular framework of **2**, as this anhydrous phase is able to adsorb up to six water molecules per cluster to lead to the hydrated derivative $[\{Cu(cyclam)\}_3SiW_{11}O_{39}Cu(H_2O)]\cdot 5H_2O$ (**2h**) without any significant alteration in its cell parameters, nor in its crystalline structure.

INTRODUCTION

Among solid-phase transitions, those in which crystalline order is retained, known as single–crystal to single–crystal (SCSC) transformations, have gathered great attention in recent years within crystal-engineering and supramolecular chemistry.[1-6] The reason why this type of transformations constitutes an increasingly studied field lays on the possibility of obtaining unprecedented compounds, which exhibit bulky properties (e.g. magnetic, catalytic, luminescent or sorptive) that can be tuned upon application of an external stimulus (e.g. heat, light, ion-exchange).[7-11] Such phase transitions allow the monitoring of how the position of atoms and molecules varies within a crystalline material when the stimuli are applied, thus providing information about the transition mechanism and its correlation with any modifica-

tion in the properties subject of interest.[12-17] As a consequence, the control of the applied stimuli offers the possibility of adjusting the response offered by these smart materials, making them suitable for performing a wide range of functions, such as molecular switches, sensors or data storage devices.[18-20]

To date, several SCSC transformations have been reported in coordination compounds such as metal-organic frameworks (MOFs),[21-23] coordination polymers[24,25] and molecular complexes,[26-28] leading to property variations as a result of the cleavage and formation of metal-to-ligand bonds. The incorporation of rigid building blocks within the framework could prevent structural collapse along the phase transition, thus facilitating the fact that the crystal retains its integrity.[29-30] For this purpose, polyoxometalates (POMs) can be considered ideal candidates because they constitute a well-known family of topologically diverse clusters based on oxygen and transitions metals with a variety of tunable properties.[31-33]

The first example of this kind of systems displaying SCSC transitions dates back to 2005, when Mizuno and collaborators analyzed the sequential and reversible thermal dehydration of $Cs_5[Cr_3O(OOCH)_6(H_2O)_3][CoW_{12}O_{40}]\cdot 7.5H_2O$. Selective adsorption of water over some other polar molecules, such as alcohols, was reported for this porous system.[34] Even though the study of crystal-to-crystal transitions is still unusual for compounds that incorporate POM anions, literature examples already cover a wide range of external stimuli able to trigger structural responses.[35] These include i) redox stimuli, as exemplified by $[C_4H_{10}NO]_{40}[W_7Mn_{12}O_{268}Si_7]$, in which the reduction of Mn^{III} ions involves modifications in the electronic properties of the system;[36] ii) light irradiation, which induces polymerization along with photochromic response in the hybrid $[Gd(NMP)_{12}(PW_{12}O_{40})][PW_{12}O_{40}]$ (NMP = N-methyl-2-pyrrolidone);[37] iii) chemical exchange, as observed in $K_2[Cr_3O(OOCH)_6(4\text{-ethylpyridine})_3]_2[\alpha\text{-}SiW_{12}O_{40}]$, which undergoes different protonation-induced SCSC transformations that allows the identification and separation of CO_2 and C_2H_4;[38,39] and iv) thermal activation, that can result in polymorphic transitions[40] or structural variations triggered by the evacuation of solvent molecules, as exemplified by a family of hybrids made of $[XW_{12}O_{40}]^{4-}$ (X = Si, Ge) anions and copper(II) complexes of bis(aminopyridil)-type ligands in which thermal dehydration induces reversible grafting of the metal-organic complexes to the POM surface or modifications on the conformation of the ligands.[41,42]

Besides the series of ionic crystals in which $[M_3O\{RCO_2\}_6L_3]^+$ macrocations (M^{III} = Cr, Fe; L = terminal ligand) are combined with Keggin-type heteropolyanions $[XM_{12}O_{40}]^{n-}$ (X = B^{III}, Si^{IV}, P^V; M = W^{VI}),[43,44] another general synthetic strategy for synthesizing POM-based compounds able to undergo SCSC transformations involves the use of copper(II) complexes of macrocyclic polyamines. The existence of available axial coordination sites, together with the plasticity of the coordination sphere of copper(II) and the ability of the macrocyclic ligands to establish a collection of cooperative supramolecular interactions with oxygen-rich POM surfaces, helps the system to avoid loss of crystallinity along the solid-state phase transition.[45] In this context, we have focused our latest studies on the $\{Cu(cyclam)\}^{2+}$ complex (cyclam = 1,4,8,11–tetraazacyclotetradecane), and reported its linking ability in a series of covalent lattices in combination with isopolyoxometalate clusters, such as heptatungstate[46] and decavanadate.[47] The former framework displays a complex dynamic response to thermal dehydration that proceeds through three consecutive SCSC transformations and involves relevant structural changes, whereas the latter constitutes a robust microporous system which remains virtually unaltered after the evacuation of water molecules. Despite the differences of their phase transition mechanisms, both systems show interesting functionalities related to POM-based hybrid networks with permanent porosity (e.g. gas sorption properties).

Recently, we extended these studies to heteropolyoxometalate-based systems and reported a full series of compounds formed by lanthanide-containing dimeric $[\{(\alpha\text{-}GeW_{11}O_{39})Ln(H_2O)(OAc)\}_2]^{12-}$ (Ln = La to Lu) anions.[48] The coordinatively unsaturated $[\{(\alpha\text{-}GeW_{11}O_{39})Ln(OAc)\}_2]^{12-}$ POM derivatives were isolated for the first time in the course of two sequential SCSC transformations that exhibited different kinetics governing their reversibility as a function of the lanthanide ion. This series exemplifies how the activated form of metal-substituted POMs bearing additional magnetic, optical or catalytic properties arising from the presence of exposed 3d- or 4f-substituting metal centers can be structurally characterized when incorporated into systems that can experience crystal dynamics.

Following with our last findings, we decided to explore further heteropolyoxometalate-based systems, and attempted the preparation of hybrid $\{Cu(cyclam)\}^{2+}$ / Keggin anion compounds to investigate whether they exhibit comparable thermostructural behavior. Here we report on the crystal dynamics of $[Cu(cyclam)(H_2O)][\{Cu(cyclam)\}_2SiW_{11}O_{39}\text{-}Cu(H_2O)]\cdot 5H_2O$ (**1**) and its thermally-triggered SCSC transformation into the anhydrous derivative $[\{Cu(cyclam)\}_3\text{-}SiW_{11}O_{39}Cu]$ (**2**). Compound **1** is made of corrugated $\{Cu(cyclam)\}^{2+}$ / $\{SiW_{11}O_{39}Cu(H_2O)\}^{6-}$ 2-dimensional covalent grids and additional $[Cu(cyclam)(H2O)]^{2+}$ counterions embedded into square-like grid voids, but dehydration fully dismantles this layered architecture to afford the neutral, discrete hybrid species found in **2**, in which the Keggin-type cluster exhibits three decorating metal-organic moieties grafted at its sur-face and must contain a 5-coordinated copper(II) center within its skeleton, therefore representing the first observation of such kind of coordinatively unsaturated cluster for metal-substituted silicotungstates in the solid state. This phase transition is irreversible, but the flexibility of the supramolecular framework in **2** allows the fast adsorption of water molecules upon air exposure to afford the hydrated $[\{Cu(cyclam)\}_3SiW_{11}O_{39}Cu\text{-}(H_2O)]\cdot 5H_2O$ (**2h**) derivative, which has also been structurally characterized by single-crystal X–ray diffraction.

EXPERIMENTAL SECTION

Materials and Methods

The precursor $K_8[SiW_{11}O_{39}]\cdot 13H_2O$ was synthesized following literature methods[49] and identified by infrared (FT–IR) spectroscopy. All other chemicals were obtained from commercial sources and used without further purification. The C, H and N were determined on a Perkin–Elmer 2400 CHN analyzer, whereas Cu content was analyzed using a Q-ICP-MS ThermoXSeries II analyzer. FT–IR spectra were obtained as KBr pellets on a SHIMADZU FTIR–8400S spectrophotome-

ter. Thermogravimetric and differential thermal analyses (TGA/DTA) were carried out from room temperature to 700 °C at a rate of 5 °C min^{-1} on a TA Instruments 2960 SDT thermobalance under a 50 cm^3 min^{-1} flow of synthetic air. Powder X-ray diffraction (PXRD) patterns were recorded in the $5 \le 2\theta \le 35°$ range (0.033° step size, 30 s per step) using a Philips X'PERT PRO diffractometer (40 kV/40 mA, θ–θ configuration) equipped with monochromated CuK$_\alpha$ radiation (λ = 1.5418 Å) and a PIXcel detector. Variable temperature PXRD patterns were collected on a Bruker D8 Advance diffractometer operating at 30 kV/20 mA and equipped with CuK$_\alpha$ radiation, a Vantec-1 PSD detector, an Anton Parr HTK2000 high-temperature furnace, and a Pt sample holder. Data sets were acquired from 30 to 890 °C every 20 °C, with a 0.16 °C s^{-1} heating rate between temperatures. The reversibility of the structural transitions was studied by a combination of PXRD and TGA/DTA analyses using crystalline samples dehydrated to 170 °C at a 2 °C min^{-1} rate under a 100 cm^3 min^{-1} flow of synthetic air, and left in contact with room moisture for different periods of time in the range from 5 to 76 h.

Table 1. Crystallographic Data for 1, 2 and 2h

	1	**2**	**2h**
formula	$C_{30}H_{86}Cu_4N_{12}O_{46}SiW_{11}$	$C_{30}H_{72}Cu_4N_{12}O_{39}SiW_{11}$	$C_{30}H_{84}Cu_4N_{12}O_{45}SiW_{11}$
fw (g mol^{-1})	3655.56	3529.46	3637.55
crystal system	monoclinic	monoclinic	monoclinic
space group	$P2_1/n$	$P2_1/n$	$P2_1/n$
a **(Å)**	14.18783(15)	14.4593(3)	14.4828(4)
b **(Å)**	21.8976(3)	22.1551(5)	22.4530(8)
c **(Å)**	23.4387(4)	20.7932(4)	20.9246(6)
α **(°)**	90	90	90
β **(°)**	97.3654(13)	91.1769(19)	90.645(3)
γ **(°)**	90	90	90
V **(Å^3)**	7221.8(2)	6659.6(3)	6803.9(4)
ρ_{calcd} **(g cm^{-3})**	3.362	3.52	3.551
μ **(mm^{-1})**	18.708	36.388	35.724
reflections			
collected	55930	52146	51046
unique (*R*$_{int}$)	14661 (0.030)	12867 (0.066)	12124 (0.101)
obs. [*I* > 2σ(*I*)]	11670	9892	7974
parameters	709	682	484
restraints	42	142	181
***R*(*F*)[a] [*I* > 2σ(*I*)]**	0.061	0.094	0.120
***wR*(*F*^{2})[b] [all]**	0.115	0.261	0.287
GoF	1.139	1.074	1.096

[a] $R(F)=\Sigma||F_o|-|F_c||/\Sigma|F_o|$; [b] $wR(F^2)=\{\Sigma[w(F_o^2-F_c^2)^2]/\Sigma[w(F_o^2)^2]\}^{1/2}$

Synthesis of $[Cu(cyclam)(H_2O)][\{Cu(cyclam)\}_2SiW_{11}O_{39}Cu(H_2O)]\cdot 5H_2O$ (1), $[\{Cu(cyclam)\}_3SiW_{11}O_{39}Cu]$ (2) and $[\{Cu(cyclam)\}_3SiW_{11}O_{39}Cu(H_2O)]\cdot 5H_2O$ (2h)

A mixture of $K_8[SiW_{11}O_{39}]\cdot 13H_2O$ (322 mg, 0.1 mmol), $Cu(CH_3CO_2)_2$ (73 mg, 0.4 mmol) and cyclam (60 mg, 0.30 mmol) was stirred for 1 h in 25 mL of water, transferred to a 50 mL Teflon-lined autoclave and kept at 140 °C for 72 h. Afterwards, the reaction mixture was cooled down to room temperature for 48 h. Compound **1** was obtained as red single-crystals suitable for X-ray diffraction. Yield: 28 mg (35% based on W). Anal. calcd (found) for $C_{30}H_{86}Cu_4N_{12}O_{46}SiW_{11}$: C, 9.91 (9.81); H, 2.25 (2.25); Cu, 6.95 (6.85); N, 4.62 (4.86). IR (cm^{-1}): 3180 (d), 3094 (d), 2909 (d), 2870 (d), 1464 (d), 1465 (m), 1430 (m),1295 (d), 1242 (d), 1003 (m), 941 (f), 895 (f), 794 (F), 741 (h), 678 (m), 532 (m), 440 (d). The anhydrous phase **2** can be obtained by heating single crystals of **1** at 120 °C in an oven for 30 min. A slight color change from red to pink was produced upon dehydration. The hydrated phase **2h** was obtained after one day of exposure of **2** to room atmosphere.

Single-Crystal X-Ray Crystallography

Crystallographic data for compounds **1, 2** and **2h** are provided in Table 1. Intensity data were collected at 100 K on a Rigaku Oxford Diffraction SuperNova diffractometer equipped with monochromated Mo Kα radiation (λ = 0.71073 Å) and Eos CCD detector in the case of **1** and Cu Kα radiation (λ = 1.54184 Å) and Atlas CCD detector for **2** and **2h**. For the measurement of **2**, single crystals of **1** were heated in an oven to 393 K at a rate of 1 K min^{-1}, and kept at this temperature for 30 min to ensure full conversion. Immediately afterwards the selected crystal was covered with Paratone® oil and placed under the N_2 stream of the diffractometer. Its temperature was set at 393 K to perform a preliminary unit cell determination and was then quenched to 100 K to proceed to the full data acquisition. Data frames were processed (unit cell determination, analytical absorption correction with face indexing, intensity data integration and correction for Lorentz and polarization effects) using the CrysAlis Pro software package.[50] The structures were solved using OLEX2[51] and refined by full–matrix least–squares with SHELXL–2014/6[52] as integrated in WinGX.[53] Data analysis was carried out using PLATON[54] for all the three structures and their visualization was performed using Crystal Maker 10.[55] Continuous shape measure (CShM) calculations were performed using SHAPE.[56]

Thermal vibrations were treated anisotropically for heavy atoms (W, Cu, Si) and POM oxygen atoms, except for **2h,** for which the O atoms of the Keggin cluster could only be refined isotropically. Hydrogen atoms of the organic ligands were placed in calculated positions and refined using a riding model with standard SHELXL parameters. In all three cases, the Cu^{II} atom from the Keggin skeleton was disordered over all the addenda metal sites except for those positions in which the terminal oxygen atom was directly attached to a metal-organic complex. The Cu^{II} occupancy factors were initially refined with no restrictions. Occupancies below 5% were then fixed to zero, leading to a total number of approx. one copper atom per POM subunit in subsequent refinements. In the last refinement cycle, the sum of the copper population factors was restricted to 1.00. The population factors of the terminal oxygen atoms belonging to mixed W/Cu positions in **2** were set equal to the corresponding W occupancies in such addenda metal sites upon assuming the presence of a coordinatively unsaturated Cu^{II} center, in good agreement with thermogravimetric analyses.

Some of the bond lengths and isotropic thermal ellipsoids of the organic ligands were normalized using SADI- and SIMU-type restraints from SHELXL. For **2h**, additional restrictions were applied to some of the Cu–N, C–C and N–C bonds (DFIX), and N–Cu–N angles (DANG) in order to model the

disorder in the metal-organic Cu1C complex. The Si atom located inside the polyoxotungstate shell was initially treated isotropically and it displayed negative ADP values originating from the poor quality of the data. We tried to overcome this problem by restraining its anisotropic thermal parameters with ISOR commands with no success. Afterwards, we opted for simulating its ADP values and equalizing them to surrounding O or W atoms using EADP-type constrains. Both methods resulted in structural models with worse agreement factors and a larger number of A-type alerts. Therefore, we decided to fix its thermal parameters manually in the final refinement cycle using those values observed for the Si atom in **1**.

In regard to water molecules of hydration, six suitable positions were located in the Fourier map of **1** and their occupancies were initially refined without restrictions. This refinement resulted in a total number of 5.3 water molecules of hydration per Keggin subunit. This number was consistent with thermogravimetric results and during the final refinement, they were accordingly fixed to 5.00. For **2h,** the much worse quality of the diffraction data allowed us to locate two positions suitable for water molecules of hydration only. The remaining water molecules were determined by thermogravimetric analyses. All of the structures show large maxima of residual electron density, which are located close to the W atoms according to the final difference density map. Large residual maxima in the final Fourier map is a common fact found in the refinement of polyoxotungstate structures due to the high absorption of heavy atoms such as W.

RESULTS AND DISCUSSION

Synthesis and Spectroscopic Characterization

Hybrid frameworks constituted by POMs and $\{Cu(cyclam)\}^{2+}$ moieties have been previously obtained by the self-assembly of both constituents in aqueous solution under mild, bench conditions.[46-47,57] However, this procedure did not succeed for $\{Cu(cyclam)\}^{2+}$ / Keggin-type anion systems. Thus, we decided to make use of hydrothermal conditions because the high temperatures and pressures associated with this synthetic method i) increase the solubility of the reactants and favors crystallization over precipitation, and ii) can induce formation of metastable phases that are otherwise inaccessible by following traditional synthetic protocols.

Compound **1** was first isolated from the hydrothermal reaction between the plenary Keggin-type $K_4[SiW_{12}O_{40}]\cdot 13H_2O$ POM salt and a threefold excess of $[Cu(cyclam)]^{2+}$ complex in aqueous medium at 140 °C under autogenous pressure for 3 days. The same temperature and reaction time conditions were previously employed by some of us in similar works to obtain single crystals suitable for X-ray diffraction of hybrid POM-based compounds with Cu^{II} complexes of N_4-donor bis(aminopyridyl) ligands.[41,42] Unfortunately, we could only obtain a reddish polycrystalline powder in a low yield of *ca.* 15 %, the preliminary characterization of which was carried out by means of FT-IR spectroscopy (Figures S1 and S2 in the Supporting Information). The presence of the $\{Cu(cyclam)\}^{2+}$ complex in the polycrystalline sample of **1** was established on the basis of its fingerprint in the metal-organic region of the spectrum above 1100 cm^{-1}.[58] The inorganic region below displayed the characteristic structure of bands of strong intensity associated with a Keggin-type POM anion, but with the vibrational bands $\nu_{as}(Si–O_c)$, $\nu_{as}(W—O_t)$, $\nu_{as}(W—O_v—W)$, and $\nu_{as}(W—O_a—W)$ at 1003, 941, 794 and 741 cm^{-1} considerably shifted in comparison with those of $[SiW_{12}O_{40}]^{4-}$, which appear at 1022, 980, 895/877 and 791 cm^{-1}, respectively. This shift, together with the presence of an additional peak ascribed to the $\nu(Cu—O)$ vibrational mode at 678 cm^{-1} unequivocally demonstrated the presence of the copper(II)-monosubstituted $[SiW_{11}O_{39}Cu(H_2O)]^{6-}$ species instead of the starting plenary α-Keggin anion in **1**. At lower wavenumber values, weaker signals attributable to $\delta(W—O_a—W)$ (532 cm^{-1}) and $\delta(W—O_v—W)$ (440 cm^{-1}) vibrations were also found.[59]

Based on these results, a mixture of the potassium salt of the monolacunary α-Keggin cluster $[SiW_{11}O_{39}]^{8-}$ (1 eq.), $Cu(CH_3CO_2)_2$ (4. eq.) and cyclam (3 eq.) were reacted to obtain compound **1** as a single-crystalline phase following a stoichiometric synthetic procedure. This reaction implies the assembly in aqueous medium between in situ generated $[SiW_{11}O_{39}Cu(H_2O)]^{6-}$ polyanion and $\{Cu(cyclam)\}^{2+}$ complexes, and allowed us to obtain reddish single crystals of **1** in a 35 % yield. It must also be highlighted that the use of the trilacunary derivative $[SiW_9O_{34}]^{10-}$ was also successful in obtaining single crystals of **1**, but the reaction yield in this case (8 %) was much lower than that of the synthetic procedure above. The identity of the crystalline products derived from these three synthetic approaches was confirmed to be compound **1** by PXRD analyses, which also evidenced their phase homogeneity (Figure S3 in the Supporting Information). Besides, the nature of the anion of the starting Cu^{II} salt (i.e. Cl^-, NO_3^-, SO_4^{2-}) did not have any effect neither on the identity of the product, nor on the reaction yields.

Thermo-Structural Behavior

To determine whether compound **1** exhibits thermo-structural behavior comparable to the framework robustness or crystal dynamics observed in our previous $\{Cu(cyclam)\}^{2+}$ / POM systems, we made use of a combination of TGA/DTA and variable-temperature (VT) PXRD experiments. Thermal decomposition of **1** (Figure S4 in the Supporting Information) occurs via three well-differentiated stages. The endothermic dehydration that extends from room temperature up to *ca.* 120 °C (experimental mass loss of 3.3 %; calcd 3.4 % for 7 H_2O molecules) is followed by a thermal stability range that indicates the presence of a stable anhydrous phase. The combustion of the cyclam ligands starts at 210 °C and it is accompanied by the breakdown of the POM framework, both processes developing via several overlapped exothermic events. The overall process accounts for the loss of three cyclam ligands per POM (experimental mass loss of 16.2 %; calcd 16.4 % for $C_{40}H_{80}N_{12}$). The mass of the final residue at ca. 610 °C is in good agreement with that expected for a sample with general formula $Cu_4O_{39}SiW_{11}$ (exp. 80.8 %; calcd. 80.3 %).

The crystalline nature of the anhydrous phase was analyzed by means of VT-PXRD measurements from 30 to 890 °C (Figure 1). The room temperature diffraction pattern of compound **1** compares well with that simulated from single-crystal XRD data, which verifies the homogeneity and purity of the crystalline phase (Figure S5 in the Supporting Information). A single thermally-dependent phase transition between crystalline states can be observed with increasing temperature, as identified by several remarkable modifications in both the positions and intensity of the diffraction maxima. More specifically, the most intense maxima of **1** located at low 2θ angles (*ca.* 7.7, 8.2 and 8.8°) vanish above 90 °C while a new crystalline phase (**2**) develops progressively

and results completely formed at 130 °C. The formation of **2** is clearly evidenced by the appearance of its most intense diffraction maximum located at 8.5°, and it should correspond to an anhydrous derivative according to the dehydration temperature in the TGA experiments. Additionally, some other less intense diffraction maxima in the 2θ ranges of 10–12°, 24–26° and 28–30° also disappear or change their position along this phase transition. The anhydrous framework **2** retains its integrity up to temperatures as high as 230 °C, above which undergoes amorphization slowly and becomes fully amorphous at temperatures above *ca.* 330 °C. These events are consistent with the stage in which the organic ligand combustion takes places in the TGA curve. The final residue above *ca.* 600 °C has been identified as a mixture of two crystalline phases: monoclinic WO_3 (PDF 88269)[60] and triclinic $CuWO_4$ (PDF 431035)[61] with Scheelite-type structure (Figure S6 in the Supporting Information). Consequently, our studies revealed compound **1** as a dynamic framework with a structural response to thermal dehydration that leads to a different crystalline state for the anhydrous phase **2**.

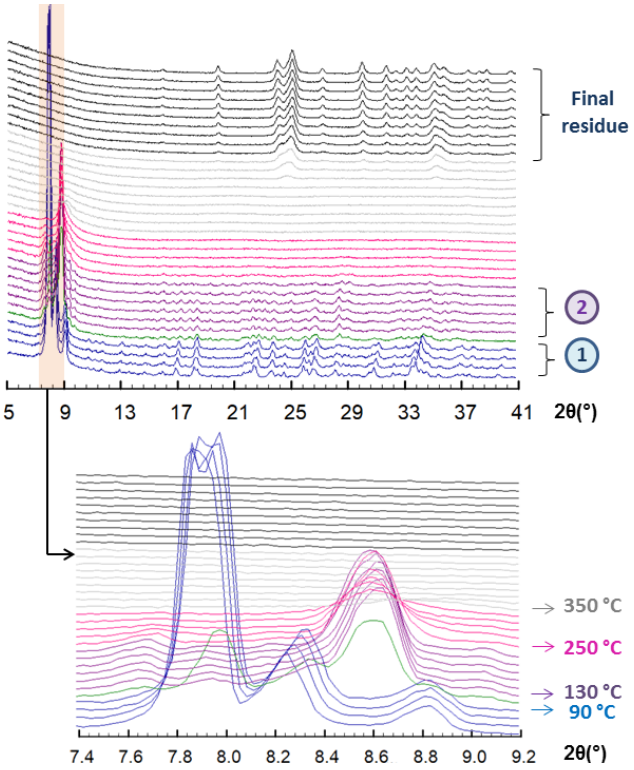

Figure 1 VT-PXRD patterns of **1** in the 30–710 °C temperature range and detail of the 2θ region from 7.4 to 9.2°.

Crystal Structure of 1

Compound **1** crystallizes in the monoclinic space group $P2_1/n$ and its asymmetric unit contains one copper(II)-monosubstituted $\{SiW_{11}O_{39}Cu(H_2O)\}^{6-}$ α-Keggin-type cluster ($SiW_{11}Cu$), three crystallographically independent metal-organic fragments located in general positions (Cu1A, Cu1B and Cu1C) and five water molecules of hydration disordered over six crystallographic positions (Figure 2). The inorganic building block consists of four edge-sharing M_3O_{13} trimers (M = W or Cu) linked to each other and to the central SiO_4 tetrahedron through corner sharing to generate a classical α-Keggin-type structure. The copper(II) atom is disordered over all the addenda M positions, except for those four connected to metal-organic fragments. No preferential site is observed for this atom because the Cu population factors of the remaining eight M positions are all between 5 and 20% (Table S2 in the Supporting Information), and therefore, no significant lengthening of the corresponding M=O_t (t = terminal) bonds is noticed. Due to this absence of preferential sites for the copper(II) center within the Keggin-type building-block, the latter has been represented as a $[SiW_{12}O_{40}]^{4-}$ plenary cluster in all of the structural figures.

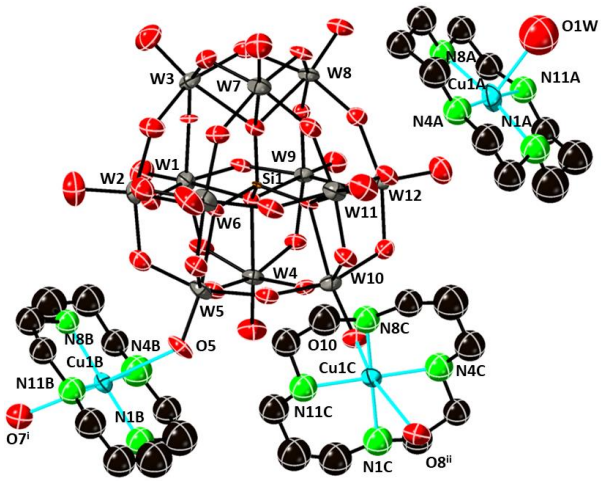

Figure 2. ORTEP representation of the asymmetric unit in **1** showing 50% probability ellipsoids, together with atom labelling scheme. Water molecules of hydration and H atoms have been omitted for the sake of clarity. Color code: W, grey; Si, orange; O, red; Cu, blue; N, green, C, black. The Cu—O and Cu—N bonds of the metal-organic complexes are highlighted in cyan. Symmetry codes: i) 3/2–*x*, 1/2+*y*, 1/2–*z*; ii) 1/2+*x*, 3/2–*y*, 1/2+*z*.

Among the three metal-organic fragments, Cu1A is a $[Cu(cyclam)(H_2O)]^{2+}$ complex acting as a charge compensating unit and displays an intermediate geometry between square-pyramidal and vacant octahedral (CShM values of 0.72 and 0.96, respectively) with the four cyclam N atoms in the basal plane and one aqua ligand (O1W) in apical position. The remaining two fragments (Cu1B and Cu1C) are $\{Cu(cyclam)\}^{2+}$ moieties grafted at the POM surface that play a bridging role between contiguous polyanions. Both Cu1B and Cu1C exhibit highly distorted octahedral geometries (CShM values in the 3.1 – 3.7 range) with the equatorial plane defined by the four N atoms from the cyclam ligand and two terminal O atoms from two adjacent Keggin units in axial positions (Figure S7 in the Supporting Information). The Jahn–Teller elongation shown by these CuN_4O_2 chromophores is remarkable as their axial bond lengths in the range of 2.704(14)–2.865(14) Å range are close to those of semi-coordination. The Cu—O and Cu—N bond lengths are compiled in Table S1 in the Supporting Information, together with the CShM values obtained upon comparison of the aforementioned geometries with the corresponding ideal polyhedra. All of the three metal-organic units (Cu1A, Cu1B and Cu1C) exhibit *trans-III* configuration, in which the N–H bonds of the two pairs of propylene-bridged N atoms point in opposite directions with respect to the CuN4 plane. This configuration has been shown to be the most favorable for

octahedral geometries according to DFT-calculations.[62] In contrast, the *trans-I* form is the most common for tetra- and penta-coordinated {TM(cyclam)}$^{2+}$ (TM = transition metal) moieties , among which only ca. 25 % of the examples deposited in the Cambridge Structural Database (CSD) adopt the *trans-III* one.[63] Regardless of the coordination geometries, we have never observed any other configuration than the *trans-III* in the collection of {Cu(cyclam)}$^{2+}$ / POM hybrids we have reported to date. From our viewpoint, this fact must be related to the way how {Cu(cyclam)}$^{2+}$ complexes interact with POM surfaces and subsequent packing effects.

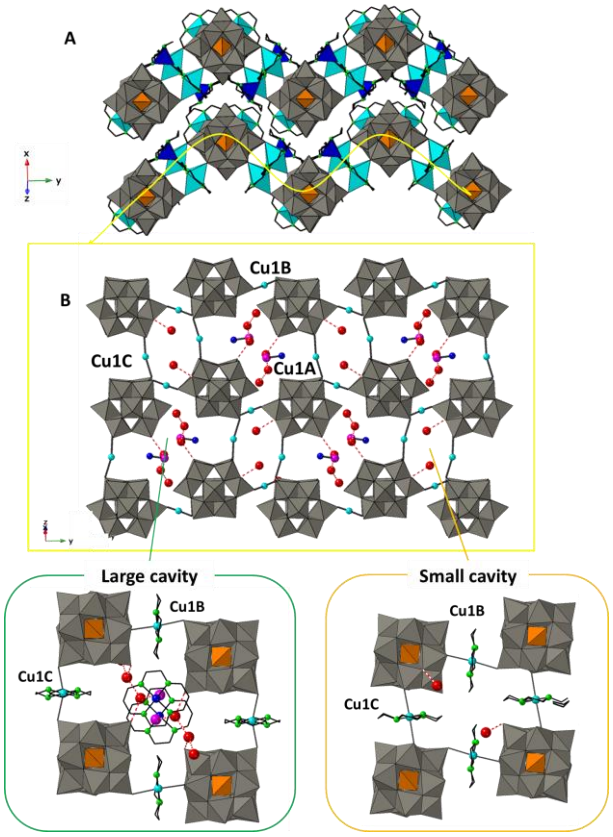

Figure 3. (A) View of the crystal packing of **1** along the [101] direction; (B) Projection of a hybrid layer in the (1 0 -1) plane (cyclam ligands omitted for the sake of clarity) and detail of the two types of grid cavities. O_W—H···O_{POM}, N—H···O_{POM} and O_W—H···O_W type interactions are represented as dashed red lines. Color code: same as in Figure 2, except for O1W (pink) and Cu1A (dark blue).

The crystal packing of **1** displays layered character as it is composed of covalent 2-dimensional hybrid assemblies stacked along the [1 0 -1] direction. These hybrid layers are constituted by $SiW_{11}Cu$ clusters linked to four adjacent counterparts though the coordination sphere of two Cu1B and two Cu1C bridging metal-organic moieties along the [0 1 0] and [1 0 1] directions, respectively. Such connectivity results in the formation of remarkably corrugated covalent grids with a corrugation angle of ca. 110° (Figure 3). Despite the long Cu—O_{POM} bonds, the intralamellar connectivity is reinforced by a set of C—H···O_{POM} and N—H···O_{POM} type contacts established between cyclam ligands and the POM surfaces. Two types of intralamellar cavities defined by four interconnected POM clusters can be found within the layers: larger, square-type and smaller, rectangular grid voids. Eight water molecules of hydration are hosted in each of the larger cavities (Cu1B···Cu1B × Cu1C···Cu1C dimensions of approx. 16 × 20 Å^2), which interact with each other and with the surfaces of the $SiW_{11}Cu$ units via several O_w—H···O_W and O_w–H···O_{POM} type hydrogen bonds. The top and bottom spaces of these rectangular grid voids are delimited by two Cu1A complexes embedded into the cavities with their apical O1W water molecules pointing directly at the inner part to participate in the hydrogen bonding network mentioned above. These moieties also play a key role in stabilizing the stacking of hybrid grids along the [1 0 -1] direction through C—H···O_{POM} and N—H···O_{POM} type contacts established with clusters from adjacent layers (Figure S8 in the Supporting Information). In contrast, each of the smaller cavities (Cu1B···Cu1B × Cu1C···Cu1C dimensions of approx. 10 × 13 Å) only incorporates two additional water molecules of hydration. The crystal packing contains also a system of parallel 1-dimensional pores of ellipsoidal section that cross the hybrid layers along the crystallographic *y* axis in undulating fashion and host all of the water molecules. These channels are direct consequence of the corrugated character of the covalent grids, and originate from the partial overlapping and subsequent communication of alternate large and small intralamellar cavities along the [010] direction thanks to corrugation. The solvent accessible space in these channels account for ca. 15 % of the unit cell volume as calculated by PLATON (Figure S8 in the Supporting Information).

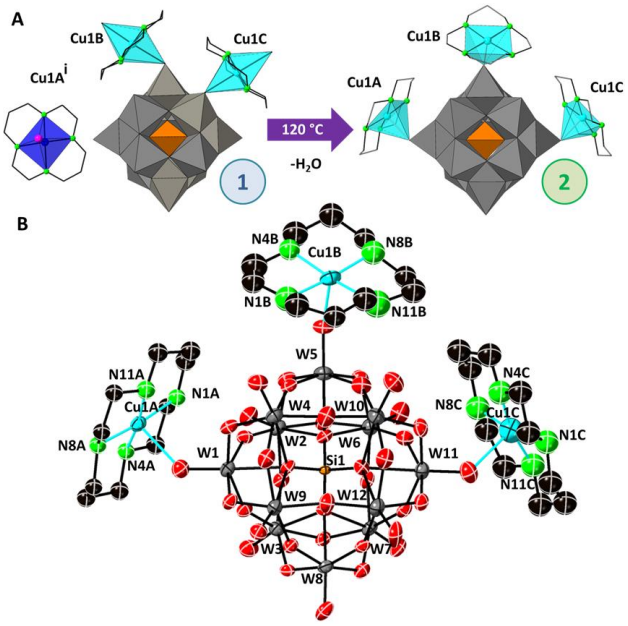

Figure 4. (A) Evolution of the Cu—O bonding scheme throughout the SCSC transformation from **1** to **2**. (B) ORTEP representation of the asymmetric unit in **2** showing 30% probability ellipsoids, together with atom labelling scheme. The H atoms have been omitted for the sake of clarity Symmetry codes: i) ½–*x*, ½+*y*, ½–*z*.

Thermally Induced SCSC Transformation into 2

To determine the structural changes associated with the thermally-triggered phase transition evidenced by VT-PXRD studies for **1**, we made use of single-crystal XRD (scXRD). Single crystals of **1** heated to 120 °C in an oven to induce

transformation, placed immediately afterwards under the N_2 stream of the diffractometer set at the same temperature, and quenched down to 100 K upon a preliminary data acquisition were employed for this purpose. Fortunately, the sample maintained its integrity as single crystal during this process, and this fact allowed us to monitor the formation and rupture of Cu—O coordination bonds throughout the phase transition that leads to the anhydrous derivative **2**.

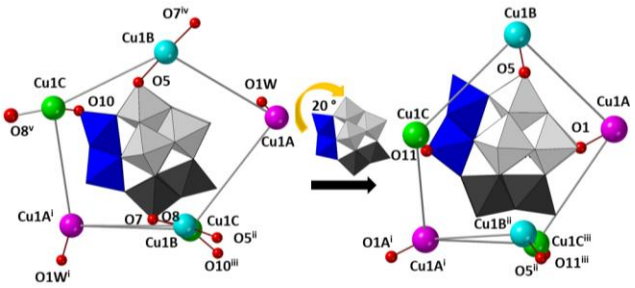

Figure 5. Schematic representation of the modifications induced in the bonding scheme of the $\{Cu(cyclam)\}^{2+}$ complexes by the rotation of the POM cluster as a result of the SCSC transformation of **1** into **2**. Two of the trimers of the Keggin anion have been highlighted in black and blue for their better visualization. Symmetry codes: i) 1/2+*x*, 1/2–*y*, –1/2+*z*; ii) 3/2–*x*, –1/2+*y*, 1/2–*z*; iii) 1/2+*x*, 1/2–*y*, 1/2+*z*; iv) 3/2–*x*, 1/2+*y*, 1/2–*z*; v) 1/2+*x*, 3/2–*y*, 1/2+*z*.

No significant modifications can be noticed upon thermal removal of water molecules neither in the crystal symmetry (the monoclinic $P2_1/n$ space group is maintained), nor in the unit cell dimensions *a* and *b*. In contrast, the parameter *c* is shortened by ca. 2.5 Å when going from **1** to **2**, along with a decrease of ca. 6° for the parameter β (Table 1). The content of the unit cell in the anhydrous phase is similar to that found for the parent hydrated compound, but for the corresponding loss of 2 coordination and 5 hydration water molecules: one copper(II)-monosubstituted Keggin-type silicotungstate cluster and three crystallographically independent metal-organic fragments (Cu1A, Cu1B, Cu1C) located in general positions (Figure 4). The Keggin-type cluster in **2** must have lost its terminal aquo ligand during dehydration and exhibit a coordinatively unsaturated copper(II) center according to thermal analyses (Figure S4 in the Supporting Information), although this fact could not be confirmed by means of crystallography due to the random disorder of the copper(II) atom over the nine addenda metal positions not linked to any metal-organic fragment within the skeleton of the $\{SiW_{11}O_{39}Cu(\_)\}^{6-}$ cluster. The loss of terminal aquo ligands is relatively common when metal-substituted POMs are transferred into non-coordinating organic solvents,[64,65] but compound **2** might constitute one of the scarce examples in the literature of such kind of coordinatively unsaturated metal-substituted Keggin skeleton observed in the solid state.[48] We tried to unequivocally prove the presence of penta-coordinated copper(II) centers with square-pyramidal $Cu(O_{POM})_5$ coordination geometry by some other experimental techniques, such as Electron Paramagnetic Resonance (EPR) spectroscopy and X-ray Photoelectron Spectroscopy (XPS), but with no success.

Removal of the apical water molecule in the coordination sphere of Cu1A and consequent grafting at a O_{POM} atom, together with rotation of the POM cluster affecting the coordination sphere of the Cu1B and Cu1C moieties, leads to the formation of neutral, discrete $[\{Cu(cyclam)\}_3SiW_{11}O_{39}Cu]$ hybrid species when **1** is transformed into the anhydrous derivative **2**. In such species, the Keggin cluster is decorated with three appended metal-organic antenna moieties, which all show tetragonally elongated square-pyramidal CuN_4O coordination environments in *trans-III* configuration (Figure 4). The relative position of all the metal-organic fragments in **2** is similar to that observed in the crystal structure of **1**, and therefore, the thermally-triggered phase transformation implies a clockwise rotation of the Keggin anion by ca. 20° around the axis parallel to the [-2 1 -1] direction (Figure 5). These changes induce the following modifications in the Cu—O bonding scheme: i) as mentioned above, Cu1A goes from acting as a $[Cu(cyclam)(H_2O)]^{2+}$ charge-compensating unit located fairly away from the POM in **1** (the shortest Cu1A···O_{POM} distance in **1** is Cu1A···O12 = 3.166(17) Å) to getting anchored to its surface upon loss of the apical water molecule (Cu1A—O1 = 2.35(2) Å in **2**); ii) the octahedral Cu1B moiety, that played a bridging role in **1** (Cu1B—O5 and Cu—$O7^a$ = 2.704(14) Å and 2.711(17) Å, respectively; symmetry code, *a*: 3/2–*x*, 1/2+*y*, 1/2–*z*), becomes a decorating appended unit by breaking one of its Cu—O_{POM} to reduce its coordination number to 5 and remain grafted to one of the clusters at the same anchoring site (Cu1B—O5 = 2.29(3) Å and Cu1B···$O7^a$ = 3.41(3) Å in **2**); and iii) Cu1C, that in the hydrated parent phase acted as a bridging moiety as well Cu1C—$O8^b$ and Cu1C—O10 = 2.865(14) and 2.762(12) Å, respectively; symmetry code, *b*: 1/2+*x*, 3/2–*y*, 1/2+*z*), undergoes modifications similar to those described for Cu1B but with an additional variation in its anchoring site upon dehydration (Cu1C—O11 = 2.29(3) Å in **2**).

In regard to the crystal packing, the covalent hybrid grids described for **1** are fully dismantled upon dehydration, so that the system dimensionality is reduced from a 2-dimensional lattice in **1** to the neutral hybrid POM species of molecular character found in **2**. The supramolecular assembly of such species is governed by a massive collection of N—H···O_{POM} and C—H···O_{POM} type contacts established between the cyclam ligands and the $\{M_4O_{18}\}$ tetrameric faces of the POM clusters. In depth analysis reveals that the three {Cu(cyclam)} decorating fragments grafted at the surface of a given Keggin unit play a donor role, whereas such unit acts as acceptor when interacting with three metal-organic fragments belonging to three adjacent tridecorated clusters; that is, each molecular $[\{Cu(cyclam)\}_3SiW_{11}O_{39}Cu]$ neutral species is connected to six contiguous counterparts (Figure 6). The overall crystal packing of **2** viewed along the crystallographic *x* axis resembles the stacking of corrugated layers described for **1**, but with a shorter interlamellar distance (Si···Si = 14.188(4) Å in **1** and 13.056(6) Å in **2**). All of these structural modifications compact the crystal packing and disrupt the system of 1-dimensional undulating pores in **1**, thereby leading to a new system of isolated small cavities that accounts for only 5.2 % of the unit cell volume according to PLATON analyses.

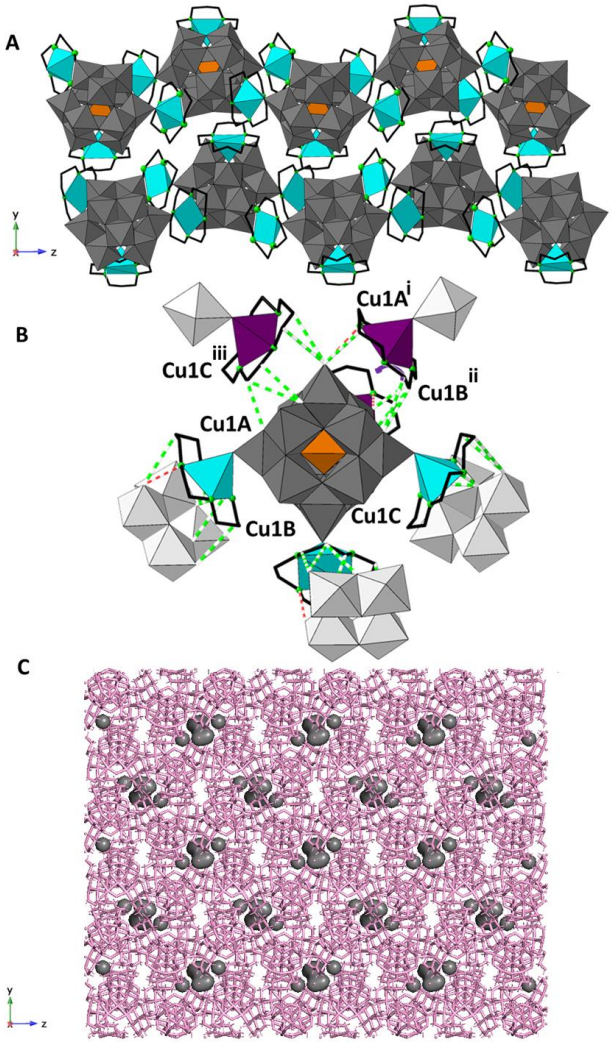

Figure 6. (A) View of the crystal packing of **2** along the crystallographic *x* axis. (B) Detail of the hydrogen bonding network established around each molecular hybrid POM species. (C). Representation of the solvent accessible cavities along the crystallographic *x* axis. Symmetry codes: i) 1–*x*, 1–*y*, 1–*z*; ii) 1+*x*, *y*, *z*; iii) 1/2+x, 1/2–*y*, 1/2+*z*.

Reversibility of the SCSC transformation

The reversibility of the SCSC transformation was studied by a combination of thermal and diffractometric analyses on different samples of **2** exposed to open air atmosphere for 5, 24 and 72 h. Thermogravimetric studies (Figure S9 in the Supporting Information) revealed that the anhydrous compound is able to adsorb a total number of 4 water molecules per cluster after five hours of exposure (calc. 2.00; found, 2.25 %). If this period of time is extended to 24 h, up to 6 water molecules per cluster incorporate into the hybrid framework, and this value represents the maximum hydration degree achievable by our system as longer exposure times (up to 72 h) did not result in an increase of the number of adsorbed water molecules (calcd 2.97; found, 2.95 %). PXRD analyses were carried out for this hydrated phase to evaluate its crystallinity and to determine whether the structure reverts back to a 2-dimensional covalent lattice upon water sorption or remains 0-dimensional based on neutral, tridecorated POM-type molecules. The diffraction pattern is shown in Figure 7, and its most intense diffraction maxima located at 2θ values in the range from 5 to 10° match exactly with those corresponding to the anhydrous phase as unequivocally evidenced by its comparison to the pattern simulated from the scXRD data of **2**. This observation demonstrates that the SCSC transformation of the 2-dimensional parent compound **1** into the 0-dimensional anhydrous derivative **2** induced by thermal dehydration is irreversible. Moreover, it also indicates that, despite its low porosity (ca. 5 % of the unit cell volume, organized as strings of isolated compartmental voids), the structure of phase **2** displays moderate ability to uptake water molecules form moisture, which must associate with flexibility of the supramolecular assembly (breathing effect) as found in some other similar networks.[66]

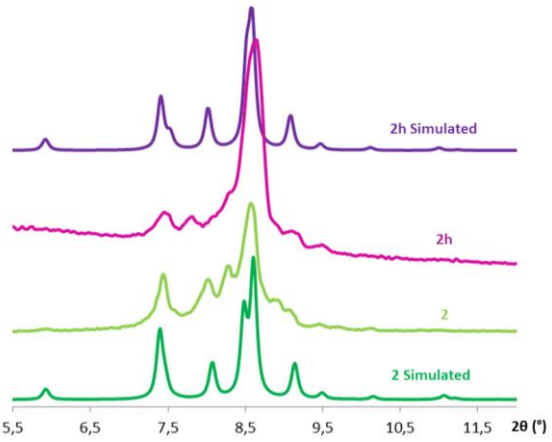

Figure 7. PXRD patterns of **2** and **2h** in the 2θ region 5.5–12° compared to those simulated from the corresponding scXRD data.

In some of our previous studies on related POM-based metal-organic hybrids, we observed that phases with very similar PXRD patterns could show remarkable bonding differences when inspected by scXRD techniques.[41,42] Therefore, we decided to carry out scXRD experiments on crystals of **2** exposed to air for 24 h regardless of their poor diffraction quality to rule out any significant modification in the structure of **2** upon water uptake to lead to the final hydrated form. Several different crystal batches were unsuccessfully tested in these experiments due to their loss of integrity and consequent cracking, but fortunately, we were able to perform one full data acquisition of enough quality for the structure of the hydrated phase to be solved. According to the experimental results (Table 1), neither the crystal symmetry nor the cell parameters are substantially altered upon water uptake and the crystal structure of the hydrated $[\{Cu(cyclam)\}_3SiW_{11}O_{39}Cu(H_2O)]\cdot 5H_2O$ form (**2h**) is indeed virtually identical to that of the anhydrous phase **2**. In the proposed molecular formula, it is assumed that one out of the six water molecules adsorbed blocks the vacant axial coordination position of the Cu^{II} atom belonging to the cluster skeleton, whereas the remaining five act as water molecules of hydration. EPR spectroscopy measurements were carried out in order to verify this assumption but, even though the signal of the Cu^{II} ions of the Keggin substituted polyanion should appear well-separated from that of Cu^{II} centers in metal-organic complexes,[67] we could only observe an average isotropic signal that prevented us from reaching any conclusion by this technique. Moreover, we were only

able to locate two out of the five crystallographic positions assumed for the water molecules of hydration. This fact is not unexpected considering the low quality of the intensity data collected. These water molecules occupy the space between the supramolecular layers that pack along the crystallographic *y* axis, which is in good agreement with the slight lengthening of the interlamellar distance (Si···Si in **2h**: = 13.091(2) Å) and the unit cell parameter *b* by ca. 0.3 Å (Figure S10 in the Supporting Information).

Taking into account the breathing effect with associated water uptake observed in **2**, gas sorption studies were attempted for this anhydrous crystalline phase. Unfortunately, the sorption capacity turned out to be extremely low for any of the two sorbates tested (N_2, CO_2) and we hypothesized whether this fact could originate from a full loss of crystallinity. These sorption studies require activation of the samples under vacuum, and therefore, we carried out PXRD analyses under similar conditions for the structural analysis of such activated sample. As shown in Figure S11 in the Supporting Information, differences can be clearly noticed when comparing the resulting diffraction pattern with that of the thermally activated anhydrous phase **2**. Although the most intense maximum at 2θ = 8.8° can still be identified, most of the diffraction maxima are vanished as a result of a considerable loss of crystallinity. This fact verifies that the vacuum dehydration mechanism results in a higher amorphization degree than that arising from thermal stimulus.

CONCLUSIONS

Hydrothermal reaction between the monolacunary α-Keggin-type polyanion $[SiW_{11}O_{39}]^{8-}$ and the $\{Cu(cyclam)\}^{2+}$ metal-organic moiety has resulted in a hybrid compound $[Cu(cyclam)(H_2O)][\{Cu(cyclam)\}_2SiW_{11}O_{39}Cu(H_2O)]\cdot 5H_2O$ (**1**), the structure of which consists in a stacking of corrugated 2-dimensional covalent grids based on copper(II)-monosubstituted Keggin-type clusters and bridging metal-organic moieties with additional complex counterions embedded into square-like grid voids. This structure is able to undergo an irreversible single-crystal-to-single-crystal transformation triggered by the thermal release of water molecules, which has been monitored by powder and single-crystal X-ray diffraction analyses. Full dehydration of **1** affords the anhydrous species $[\{Cu(cyclam)\}_3SiW_{11}O_{39}Cu]$ (**2**) through a process that involves simultaneous formation and cleavage of $Cu–O_{POM}$ bonds induced by the rotation of the Keggin clusters. These changes result in the full dismantling of the parent covalent framework, which reduces the structure dimensionality to discrete, neutral POM-based tridecorated molecular species, what constitutes the first example in which such type of transition from a 2-dimensional to a 0-dimensional system is observed in POM-metalorganic hybrid compounds. The great flexibility of the supramolecular structure of **2** has been evidenced by a combination of diffractometric and thermal studies, which showed up the ability of the anhydrous phase to adsorb up to six water molecules per cluster to lead to the hydrated derivative $[\{Cu(cyclam)\}_3SiW_{11}O_{39}Cu(H_2O)]\cdot 5H_2O$ (**2h**) with no significant alterations in its cell parameters, nor in its crystalline structure.

ASSOCIATED CONTENT

Supporting Information

FT-IR spectra, PXRD patterns, TGA/DTA curves, structural figures, and tables (PDF). This material is available free of charge via the Internet at http://pubs.acs.org. CCDC 1987978 (**1**), 1987979 (**2**) and 1987980 (**2h**) contain the supplementary crystallographic data for this paper. These data are provided free of charge by The Cambridge Crystallographic Data Centre.

AUTHOR INFORMATION

Corresponding Author

* E-mail: benat.artetxe@ehu.eus (B.A.)
* E-mail: juanma.zorrilla@ehu.es (J.M.G.-Z.)

ORCID

Beñat Artetxe: 0000-0002-7373-4596
Santiago Reinoso: 0000-0001-8329-5972
Juan M. Gutiérrez-Zorrilla: 0000-0001-8777-8533

Author Contributions

The manuscript was written through contributions of all authors. All authors have given approval to the final version of the manuscript.

Funding Sources

This work was funded by Eusko Jaurlaritza/Gobierno Vasco (EJ/GV, grants IT1291-19 and PIBA2018-59) and Ministerio de Ciencia, Innovación y Universidades (grant MAT2017-89553-P). L.F.N. and E.R.B. are indebted to EJ/GV for their predoctoral fellowships (PRE_2019_1_0106 and PRE_2018_1_0143).

Notes

The authors declare no competing financial interests.

ACKNOWLEDGMENTS

Technical and human support provided by SGIker (UPV/EHU) is gratefully acknowledged.

REFERENCES

(1) Vittal, J. J. Supramolecular Structural Transformations Involving Coordination Polymers in the Solid State. *Coord. Chem. Rev.* **2007**, *251*, 1781–1795.

(2) Zhang, X.; Vieru, V.; Feng, X.; Liu, J.-L.; Zhang, Z.; Na, B.; Shi, W.; Wang, B.-W.; Powell, A. K.; Chibotaru, L. F.; Gao, S.; Cheng, P.; Long, J. R. Influence of Guest Exchange on the Magnetization Dynamics of Dilanthanide Single-Molecule-Magnet Nodes within a Metal-Organic Framework. *Angew. Chem. Int. Ed.* **2015**, *54*, 9861–9865.

(3) Du, M.; Li, C.-P.; Wu, J.-M.; Guo, J.-H.; Wang, G.-C. Destruction and Reconstruction of the Robust $[Cu_2(OOCR)_4]$ Unit during Crystal Structure Transformations between Two Coordination Polymers. *Chem. Commun.* **2011**, *47*, 8088–8090.

(4) Park, I.-H.; Chanthapally, A.; Lee, H.-H.; Quah, H. S.; Lee, S. S.; Vittal, J. J. Solid-State Conversion of a MOF to a Metal-Organo Polymeric Framework (MOPF) via [2+2] Cycloaddition Reaction. *Chem. Commun.* **2014**, *50*, 3665–3667.

(5) Wang, C.; Li, L.; Bell, J. G.; Lv, X.; Tang, S.; Zhao, X.; Thomas, K. M. Hysteretic Gas and Vapor Sorption in Flexible Interpenetrated Lanthanide-Based Metal–Organic Frame-

works with Coordinated Molecular Gating via Reversible Single-Crystal-to-Single-Crystal Transformation for Enhanced Selectivity. *Chem. Mater*. **2015**, *27*, 1502–1516.

(6) Zhang, J.-P.; Liao, P.-Q.; Zhou, H.-L.; Lin, R.-B.; Chen, X.-M. Single-Crystal X-ray Diffraction Studies on Structural Transformations of Porous Coordination Polymers. *Chem. Soc. Rev*. **2014**, *43*, 5789–5814.

(7) Lee, E.; Kim, Y.; Heo, J.; Park, K.-M. 3D Metal–Organic Framework Based on a Lower-Rim Acid-Functionalized Calix[4]arene: Crystal-to-Crystal Transformation upon Lattice Solvent Removal. *Cryst. Growth Des.* **2015**, *15*, 3556–3560.

(8) Lv, G.-C.; Wang, P.; Liu, Q.; Fan, J.; Chen, K.; Sun, W.-Y. Unprecedented Crystal Dynamics: Reversible Cascades of Single-Crystal-to-Single-Crystal Transformations. *Chem. Commun*. **2012**, *48*, 10249–10251.

(9) Zhang, S.; Qu, X.-N.; Xie, G.; Wei, Q.; Chen, S.-P. Syntheses, Structural Analyses and Luminescent Property of Four Alkaline-Earth Coordination Polymers. *J. Solid State Chem*. **2014**, *210*, 36–44.

(10) Liu, Z.-Y.; Yang, E.-C.; Li, L.-L.; Zhao, X.-J. A Reversible SCSC Transformation from a Blue Metamagnetic Framework to a Pink Antiferromagnetic Ordering Layer Exhibiting Concomitant Solvatochromic and Solvatomagnetic Effects. *Dalton Trans*. **2012**, *41*, 6827-6832.

(11) Efthymiou, C. G.; Kyprianidou, E. J.; Milios, C. J.; Manos, M. J.; Tasiopoulos, A. J. Flexible Lanthanide MOFs as Highly Selective and Reusable Liquid MeOH Sorbents. *J. Mater. Chem. A* **2013**, *1*, 5061–5069.

(12) Campo, J.; Falvello, L. R.; Mayoral, I.; Palacio, F.; Soler, T.; Tomas, M. Reversible Single-Crystal-to-Single-Crystal Cross-Linking of a Ribbon of Cobalt Citrate Cubanes to Form a 2D Net. *J. Am. Chem. Soc*. **2008**, *130*, 2932–2933.

(13) Ho, T.-Y.; Huang, S.-M.; Wu, J.-Y.; Hsu, K.-C.; Lu, K.-L. Direct Guest Exchange Induced Single-Crystal to Single-Crystal Transformation Accompanying Irreversible Crystal Expansion in Soft Porous Coordination Polymers. *Cryst. Growth Des.* **2015**, *15*, 4266–4271.

(14) He, Y.-C.; Yang, J.; Liu, Y.-Y.; Ma, J.-F. Series of Solvent-Induced Single-Crystal to Single-Crystal Transformations with Different Sizes of Solvent Molecules. *Inorg. Chem*. **2014**, *53*, 7527–7533.

(15) Sarma, D.; Natarajan, S. Usefulness of in Situ Single Crystal to Single Crystal Transformation (SCSC) Studies in Understanding the Temperature-Dependent Dimensionality Cross-over and Structural Reorganization in Copper-Containing Metal–Organic Frameworks (MOFs). *Cryst. Growth Des.* **2011**, *11*, 5415–5423.

(16) Khullar, S.; Mandal, S. K. Supramolecular Assemblies of Dimanganese Subunits and Water Clusters Organized by Strong Hydrogen Bonding Interactions: Single Crystal to Single Crystal Transformation by Thermal De-/Rehydration Processes. *Cryst. Growth Des.* **2012**, *12*, 5329–5337.

(17) Kim, Y.; Das, S.; Bhattacharya, S.; Hong, S.; Kim, M. G.; Yoon, M.; Natarajan, S.; Kim, K. Metal-Ion Metathesis in Metal–Organic Frameworks: A Synthetic Route to New Metal–Organic Frameworks. *Chem. Eur. J*. **2012**, *18*, 16642–16648.

(18) Asha, K. S.; Bhattacharjee, R.; Mandal, S. Complete Transmetalation in a Metal–Organic Framework by Metal Ion Metathesis in a Single Crystal for Selective Sensing of Phosphate Ions in Aqueous Media. *Angew. Chem. Int. Ed.* **2016**, *55*, 11528-11532.

(19) Huang, C.; Wu, J.; Song, C.; Ding, R.; Qiao, Y.; Hou, H.; Chang, J.; Fan, Y. Reversible Conversion of Valence-Tautomeric Copper Metal–Organic Frameworks Dependent Single-Crystal-to-Single-Crystal Oxidation/Reduction: A Redox-Switchable Catalyst for C–H Bonds Activation Reaction. *Chem. Commun*. **2015**, *51*, 10353-10356.

(20) Li, F. F.; Zhang, L.; Gong, L. L.; Yan, C. S.; Gao, H. Y.; Luo, F. Reversible Photo/Thermoswitchable Dual-Color Fluorescence through Single-Crystal-to-Single-Crystal Transformation. *Dalton Trans.* **2017**, *46*, 338-341.

(21) Fan, W.; Lin, H.; Yuan, X.; Dai, F.; Xiao, Z.; Zhang, L.; Luo, L.; Wang, R. Expanded Porous Metal–Organic Frameworks by SCSC: Organic Building Units Modifying and Enhanced Gas-Adsorption Properties. *Inorg. Chem*. **2016**, 55, 6420-6425.

(22) Hao, Z.-M.; Zhang, X.-M. Solvent Induced Molecular Magnetic Changes Observed in Single-Crystal-to-Single-Crystal Transformation. *Dalton Trans.* **2011**, *40*, 2092-2098.

(23) Ansari, S. N.; Verma, S. K.; Garin, A. A.; Mobin, S. M. Vacuum-Mediated Single-Crystal-to-Single-Crystal (SCSC) Transformation in Na-MOFs: Rare to Novel Topology and Activation of Nitrogen in Triazole Moieties. *Cryst. Growth Des.* **2018**, *18*, 1287-1292.

(24) Anderson, S. L.; Gładysiak, A.; Boyd, P. G.; Ireland, C. P.; Miéville, P.; Tiana, D.; Vlaisavljevich, B.; Schouwink, P.; van Beek, W.; Gagnon, K. J.; Smit, B.; Stylianou, K. C. Formation Pathways of Metal–Organic Frameworks Proceeding through Partial Dissolution of the Metastable Phase. *CrystEngComm*. **2017**, *19*, 3407-3413.

(25) Ke, S.-Y.; Wang, C.-C. Water-Induced Reversible SCSC or Solid-State Structural Transformation in Coordination Polymers. *CrystEngComm*. **2015**, *17*, 8776-8785.

(26) Hu, F.-L.; Shi, Y.-X.; Chen, H.-H.; Lang, J.-P. A Zn(II) Coordination Polymer and its Photocycloaddition Product: Syntheses, Structures, Selective Luminescence Sensing of Iron(III) Ions and Selective Absorption of Dyes. *Dalton Trans.* **2015**, *44*, 18795–18803.

(27) Shen, P.; He, W.-W.; Du, D.-Y.; Jiang, H.-L.; Li, S.-L.; Lang, Z.-L.; Su, Z.-M.; Fu, Q.; Lan, Y.-Q. Solid-State Structural Transformation Doubly Triggered by Reaction Temperature and Time in 3D Metal-Organic Frameworks: Great Enhancement of Stability and Gas Adsorption. *Chem. Sci.* **2014**, *5*, 1368–1374.

(28) Choi, S. B.; Furukawa, H.; Nam, H. J.; Jung, D.-Y.; Jhon, Y. H.; Walton, A.; Book, D.; O'Keeffe, M.; Yaghi, O. M.; Kim, J. Reversible Interpenetration in a Metal–Organic Framework Triggered by Ligand Removal and Addition. *Angew. Chem. Int. Ed*. **2012**, *51*, 8791–8795.

(29) Rosi, N. L.; Eddaoudi, M.; Kim, J.; O'Keeffe, M.; Yaghi, O. M. Infinite Secondary Building Units and Forbidden Catenation in Metal-Organic Frameworks. *Angew. Chem. Int. Ed*. **2002**, *41*, 284–287.

(30) Cai, L.-Z.; Jiang, X.-M.; Zhang, Z.-J.; Guo, P.-Y.; Jin, A.-P.; Wang, M.-S.; Guo, G.-C. Reversible Single-Crystal-to-Single-Crystal Transformation and Magnetic Change of Nonporous Copper(II) Complexes by the Chemisorption/Desorption of HCl and H_2O. *Inorg. Chem*. **2017**, *56*, 1036–1040.

(31) Pope, M. T. Heteropoly and Isopoly Oxometalates; Springer: Berlin, Germany, 1983.

(32) *Polyoxometalate Chemistry: from Topology via Self–Assembly to Applications*; Pope, M. T., Müller, A., Eds.; Kluwer: Dordrecht, The Netherlands, 2001.

(33) *Polyoxometalate Molecular Science*, Borrás-Almenar, J. J.; Coronado, E.; Müller A.; Pope, M. T. Eds.; Kluwer: Dordrecht, The Netherlands, 2003.

(34) Uchida, S.; Mizuno, N. Zeotype Ionic Crystal of $Cs_5[Cr_3O(OOCH)_6(H_2O)_3][\alpha\text{-}CoW_{12}O_{40}]\cdot 7.5H_2O$ with Shape-Selective Adsorption of Water. *J. Am. Chem. Soc*. **2004**, *126*, 1602-1603.

(35) Reinoso, S.; Artetxe, B.; San Felices, L.; Gutiérrez-Zorrilla, J. M. Single-Crystal-to-Single-Crystal Transformations in Stimuli-Responsive Compounds Based on Polyoxometalate Clusters. In *Polyoxometalates: Properties, Structure and Synthesis;* Roberts, A. P., Ed.; Nova Science Publishers: Hauppauge, NY, USA; 2016; pp. 143-212.

(36) Thiel, J.; Ritchie, C.; Streb, C.; Long, D.L.; Cronin, L. Heteroatom-Controlled Kinetics of Switchable Polyoxometalate Frameworks. *J. Am. Chem. Soc.* **2009**, *131*, 4180-4181.

(37) Zhang, L.-Z.; Gu, W.; Liu, X.; Dong, Z.; Li, B. Solid-State Photopolymerization of a Photochromic Hybrid Based on Keggin Tungstophosphates. *CrystEngComm* **2008**, *10*, 652-654.

(38) Uchida, S.; Takahashi, E.; Mizuno, N. Porous Ionic Crystals Modified by Post-Synthesis of $K_2[Cr_3O(OOCH)_6(etpy)_3]_2[\alpha\text{-}SiW_{12}O_{40}]\cdot 8H_2O$ through Single-Crystal-to-Single-Crystal Transformation. *Inorg. Chem.* **2013**, *52*, 9320-9326.

(39) Eguchi, R.; Uchida, S.; Mizuno, N. Inverse and High CO_2/C_2H_2 Sorption Selectivity in Flexible Organic–Inorganic Ionic Crystals. *Angew. Chem. Int. Ed.* **2012**, *51*, 1635–1639.

(40) Barats-Damatov, D; Shimon, L. J. V.; Feldman, Y.; Bendikov, T.; Neuman, R. Solid-State Crystal-to-Crystal Phase Transitions and Reversible Structure–Temperature Behavior of Phosphovanadomolybdic Acid, $H_5PV_2Mo_{10}O_{40}$. *Inorg. Chem.* **2015**, *54*, 628-634.

(41) Iturrospe, A.; Artetxe, B.; Reinoso, S.; San Felices L.; Vitoria, P.; Lezama, L.; Gutiérrez-Zorrilla, J. M. Copper(II) Complexes of Tetradentate Pyridyl Ligands Supported on Keggin Polyoxometalates: Single-Crystal to Single-Crystal Transformations Promoted by Reversible Dehydration Processes. *Inorg. Chem.* **2013**, 52, 3084-3093.

(42) Iturrospe, A.; San Felices, L.; Reinoso, S.; Artetxe, B.; Lezama, L.; Gutiérrez-Zorrilla, J. M. Reversible Dehydration in Polyoxometalate-Based Hybrid Compounds: A Study of Single-Crystal to Single-Crystal Transformations in Keggin-Type Germanotungstates Decorated with Copper(II) Complexes of Tetradentate N-Donor Ligands. *Cryst. Growth Des.* **2014**, *145*, 2318-2328.

(43) Uchida, S.; Mizuno, N. Design and Syntheses of Nano-Structured Ionic Crystals with Selective Sorption Properties. *Coord. Chem. Rev.* **2007**, *251*, 2537–2546. and references therein.

(44) Eguchi, R.; Uchida, S.; Mizuno, N. Highly Selective Sorption and Separation of CO_2 from a Gas Mixture of CO_2 and CH_4 at Room Temperature by a Zeolitic Organic–Inorganic Ionic Crystal and Investigation of the Interaction with CO_2. *J. Phys. Chem. C* **2012**, *116*, 16105–16110.

(45) Reinoso, S.; Artetxe, B.; Gutiérrez-Zorrilla, J. M. Single-Crystal-to-Single-Crystal Transformations Triggered by Dehydration in Polyoxometalate-Based Compounds. *Acta Crystallogr. Sect. C* **2018**, *C74*, 1222–1242.

(46) Martín-Caballero, J.; Artetxe, B.; Reinoso, S.; San Felices, L.; Castillo, O.; Beobide, G.; Vilas, J. L.; Gutiérrez-Zorrilla, J. M. Thermally-Triggered Crystal Dynamics and Permanent Porosity in the First Heptatungstate-Metalorganic Three-Dimensional Hybrid Framework. *Chem. Eur. J.* **2017**, *23*, 14962-14974.

(47) Martín-Caballero, J.; San José Wéry, A. ; Reinoso, S.; Artetxe, B.; San Felices, L.; El Bakkali, B.; Trautwein, G.; Alcañiz-Monge, J.; Vilas, J. L.; Gutiérrez-Zorrilla, J. M. A Robust Open Framework Formed by Decavanadate Clusters and Copper(II) Complexes of Macrocyclic Polyamines: Permanent Microporosity and Catalytic Oxidation of Cycloalkanes. *Inorg. Chem.* **2016**, 55, 4970–4979.

(48) Martín-Caballero, J.; Artetxe, B. Reinoso, S.; San Felices, L. Vitoria, P.; Larrañaga, A.; Vilas, J. L.; Gutierrez-Zorrilla, J. M. Thermostructural Behavior in a Series of Lanthanide-Containing Polyoxotungstate Hybrids with Copper(II) Complexes of the Tetraazamacrocycle Cyclam: A Single-Crystal-to-Single-Crystal Transformation Study. *Inorg. Chem*. **2019**, *58*, 4365-4375.

(49) Tézé, A.; Hervé, G. Early Transition Metal Polyoxoanions. *Inorg. Synth.* **1990**, *27*, 85–96.

(50) *CrysAlisPro Software System*, Version 171.37.34; Agilent Technologies UK Ltd.: Oxford, UK, 2012.

(51) Dolomanov, O. V.; Bourhis, L. J.; Gildea, R. J.; Howard, J. A. K.; Puschmann, H. OLEX2: A Complete Structure Solution, Refinement and Analysis Program. *J. Appl. Crystallogr.* **2009**, *42*, 339–341.

(52) Sheldrick, G. M. Crystal Structure Refinement with SHELXL. *Acta Crystallogr. Sect. C* **2015**, *C71*, 3–8.

(53) Farrugia, L. J. WinGX Suite for Small-Molecule Single-Crystal Crystallography. *J. Appl. Crystallogr.* **1999**, *32*, 837–838.

(54) Spek, A. L. Structure Validation in Chemical Crystallography. *Acta Crystallogr. Sect. D* **2009**, *D65*, 148–155.

(55) Palmer, D. C. CrystalMaker; CrystalMaker Software Ltd: Oxford, UK, 2014.

(56) Alvarez, S.; Avnir, D.; Llunell, M.; Pinsky, M. Continuous Symmetry Maps and Shape Classification. The Case of Six-Coordinated Metal Compounds. *New J. Chem.* **2002**, *26*, 996-1009.

(57) Martín-Caballero, J.; San José Wéry, A.; Artetxe, B.; Reinoso, S.; San Felices, L.; Vilas, J. L.; Gutiérrez-Zorrilla, J. M. Sequential Single-Crystal-to-Single-Crystal Transformations Promoted by Gradual Thermal Dehydration in a Porous Metavanadate Hybrid. *CrystEngComm* **2015,** *17*, 8915-8925.

(58) Bounsall, E. J.; Koprich, S. R.; Synthesis and Characterization of Cyclam Complexes of Rhodium(III). *Can. J. Chem.* **1970**, *48*, 1481-1491.

(59) San Felices, L.; Vitoria, P.; Gutiérrez-Zorrilla, J. M.; Lezama, L.; Reinoso, S. Hybrid Inorganic–Metalorganic Compounds Containing Copper(II)-Monosubstituted Keggin Polyanions and Polymeric Copper(I)Complexes. *Inorg. Chem.* **2006**, *45*, 7748–7757.

(60) Woodward, P. M.; Sleight, A.W.; Vogt, T. Structural Refinement of Triclinic Tungsten Oxide. *J. Phys. Chem. Solids* **1995**, *56*, 1305-13015.

(61) Schofield, P. F.; Knight, K. S.; Redfern, S. A. T.; Cressey, G. Distortion Characteristics Across the Structural Phase Transition in $(Cu_{1-x}Zn_x)WO_4$. *Acta Crystallogr. Sect. B* **1997**, *B53*, 102-112.

(62) Bakaj, M.; Zimmer, M. Conformational Analysis of Copper(II) 1,4,8,11-Tetraazacyclotetradecane Macrocyclic Systems. *J. Mol. Struct.* **1999**, *508*, 59-72.

(63) Groom, C.R.; Bruno, I.J.; Lightfoot, M.P.; Ward, S.C. The Cambridge Structural Database. *Acta Crystallogr. Sect. B* **2016**, *B72*, 171–179.

(64) Giraldi, M.; Blanchard, S.; Griveau, S.; Simon, P.; Fontecave, M.; Bedioui, F.; Proust, A. Electro-Assisted Reduction of CO_2 to CO and Formaldehyde by $(TOA)_6[\alpha\text{-}SiW_{11}O_{39}Co(\_)]$ Polyoxometalate. *Eur. J. Inorg. Chem*. **2015**, 3642–3648.

(65) Szczepankiewicz, S. H.; Ippolito, C. M.; Santora, B. P.; Van de Ven, T. J.; Ippolito, G. A.; Fronckowiak, L.; Wiatrowski, F.; Power, T.; Kozik, M. Interaction of Carbon Dioxide with Transition-Metal-Substituted Heteropolyanions in Nonpolar Solvents. Spectroscopic Evidence for Complex Formation. *Inorg. Chem.* **1998**, *37*, 4344-4352.

(66) Uchida, S.; Hashimoto, M.; Mizuno, N. A Breathing Ionic Crystal Displaying Selective Binding of Small Alcohols and Nitriles: $K_3[Cr_3O(OOCH)_6(H_2O)_3][\alpha\text{-}SiW_{12}O_{40}]$ $16H_2O$. *Angew. Chem. Int. Ed.* **2002**, *41*, 2814-2817.

(67) Reinoso, S.; Vitoria, P.; San Felices, L.; Lezama, L.; Gutiérrez-Zorrilla, J.M. Organic–Inorganic Hybrids Based on Novel Bimolecular $[Si_2W_{22}Cu_2O_{78}(H_2O)]^{12-}$ Polyoxometalates and the Polynuclear Complex Cations $[Cu(ac)(phen)(H_2O)]_n^{n+}$ (n=2, 3). *Chem. Eur. J.* **2005**, *11*, 1538–1548.

For Table of Contents Use Only

Thermally-Induced Structural Transitions between Single-Crystalline States in the First Hybrid Compound Combining Keggin-Type Clusters with Metal-Cyclam Complexes: From 2-Dimensional Covalent Assemblies to Discrete Molecular Species

Leticia Fernández-Navarro, Amaia Iturrospe, Santiago Reinoso, Beñat Artetxe, Estibaliz Ruiz-Bilbao, Leire San Felices, and Juan M. Gutiérrez–Zorrilla.

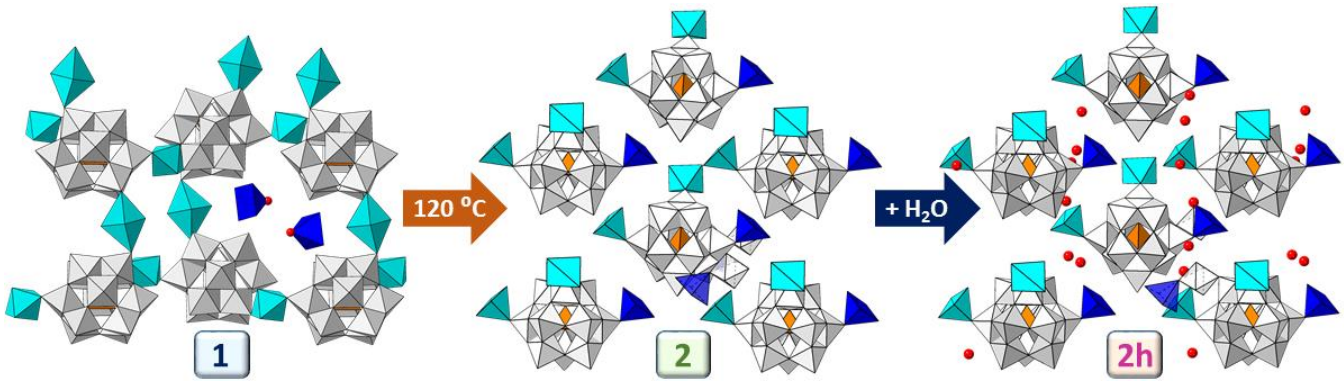

Synopsis: The 2-dimensional covalent framework $[Cu(cyclam)(H_2O)][\{Cu(cyclam)\}_2SiW_{11}O_{39}Cu(H_2O)]\cdot 5H_2O$ (**1**) undergoes a thermally-triggered single-crystal to single-crystal transformation that involves not only the release of water molecules, but also the cleavage and formation of Cu—O bonds induced by the rotation of Keggin clusters. These modifications afford the anhydrous $[SiW_{11}O_{39}Cu\{Cu(cyclam)\}_3]$ (**2**) 0-dimensional derivative in which the Keggin skeleton displays a coordinatively unsaturated copper(II) ion. Phase **2** adsorbs up to six water molecules to lead to the hydrated form **2h** without structural alterations due to the great flexibility of its supramolecular network.

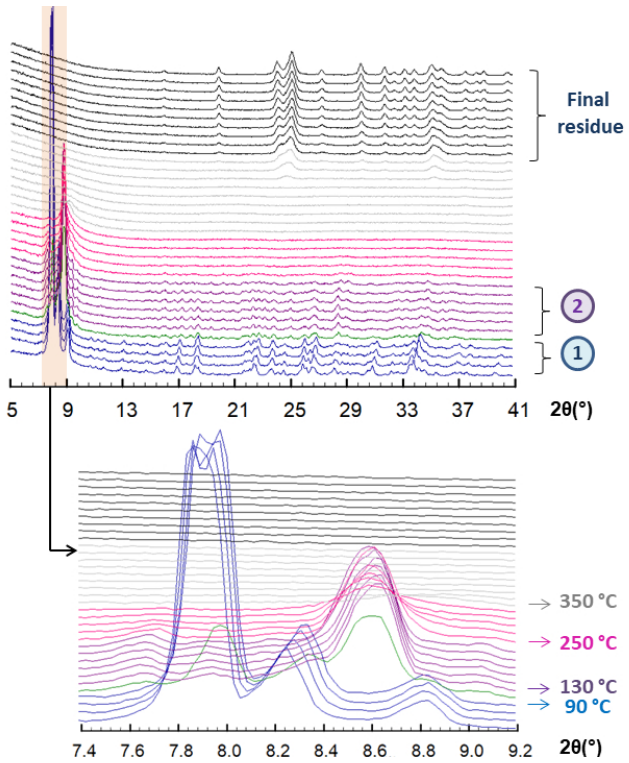

254x190mm (96 x 96 DPI)

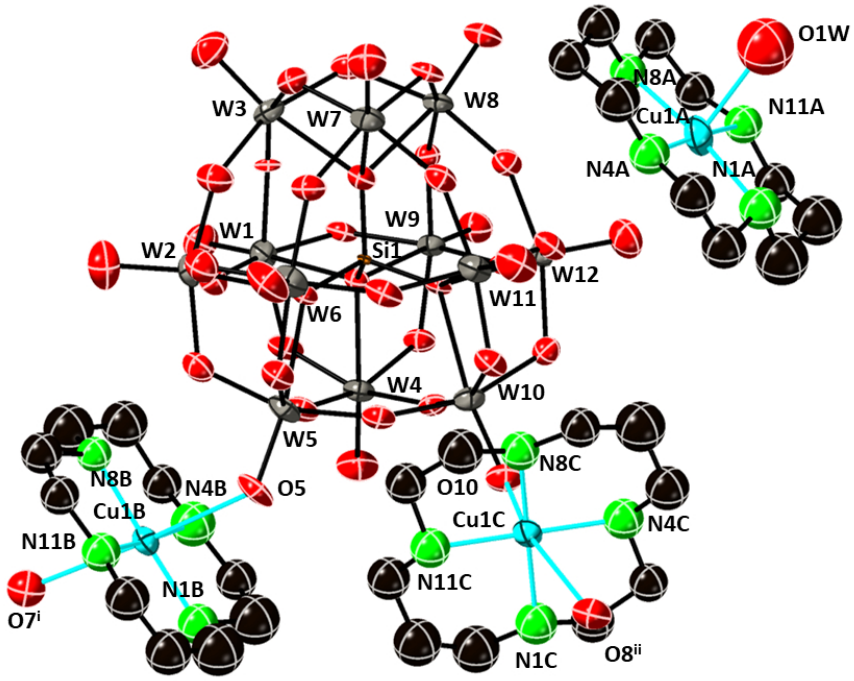

254x190mm (96 x 96 DPI)

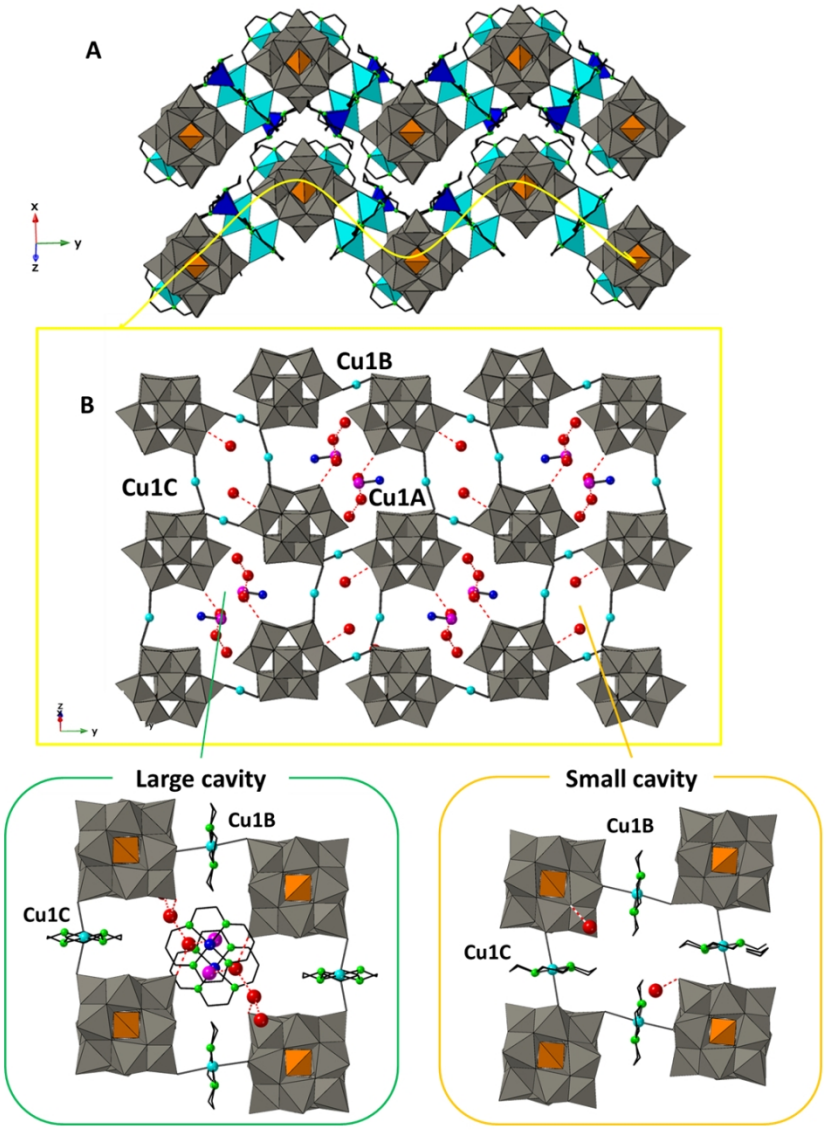

286x400mm (96 x 96 DPI)

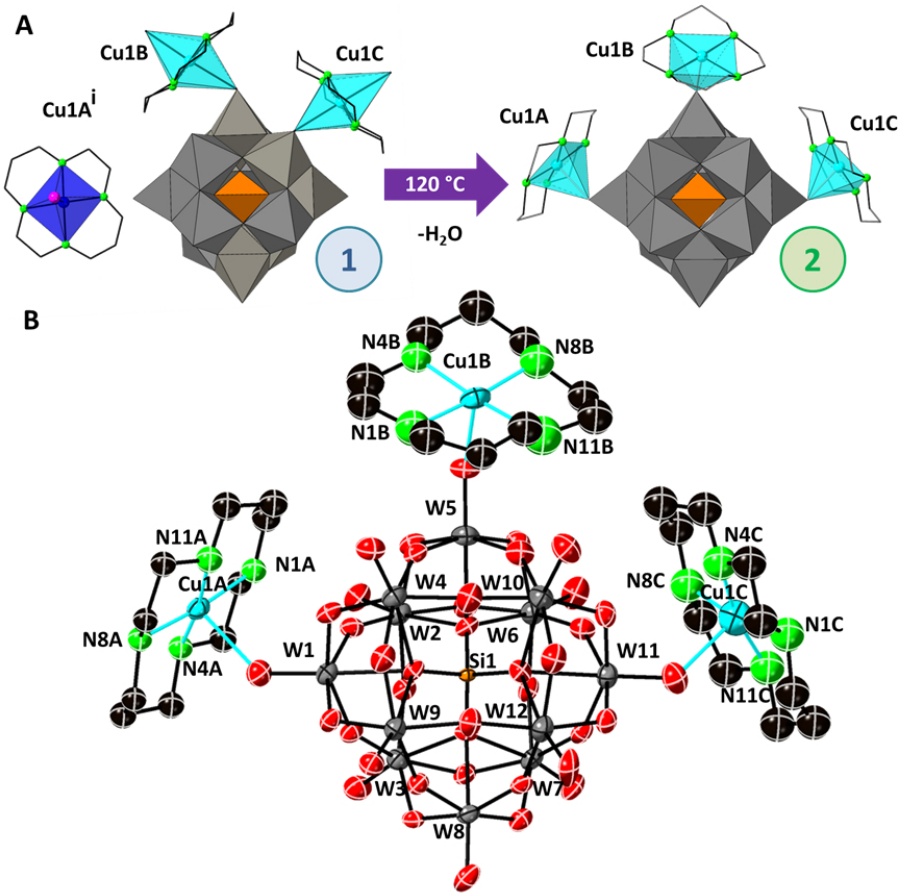

254x259mm (96 x 96 DPI)

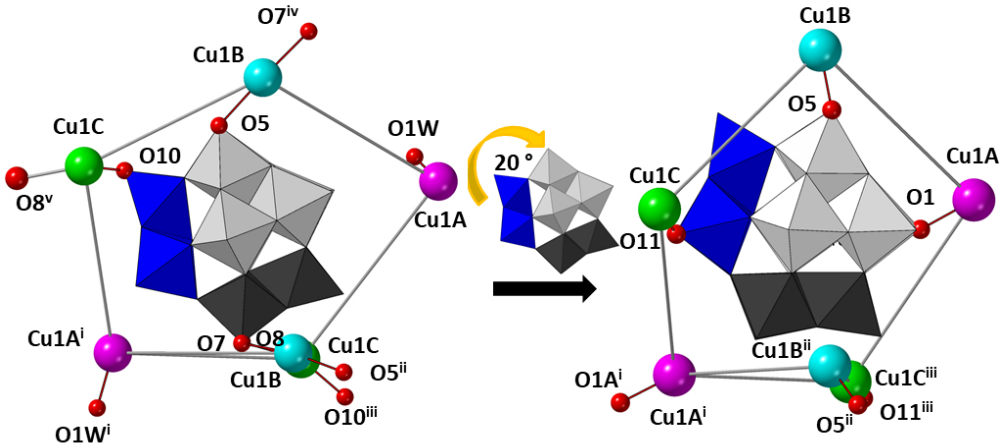

269x210mm (96 x 96 DPI)

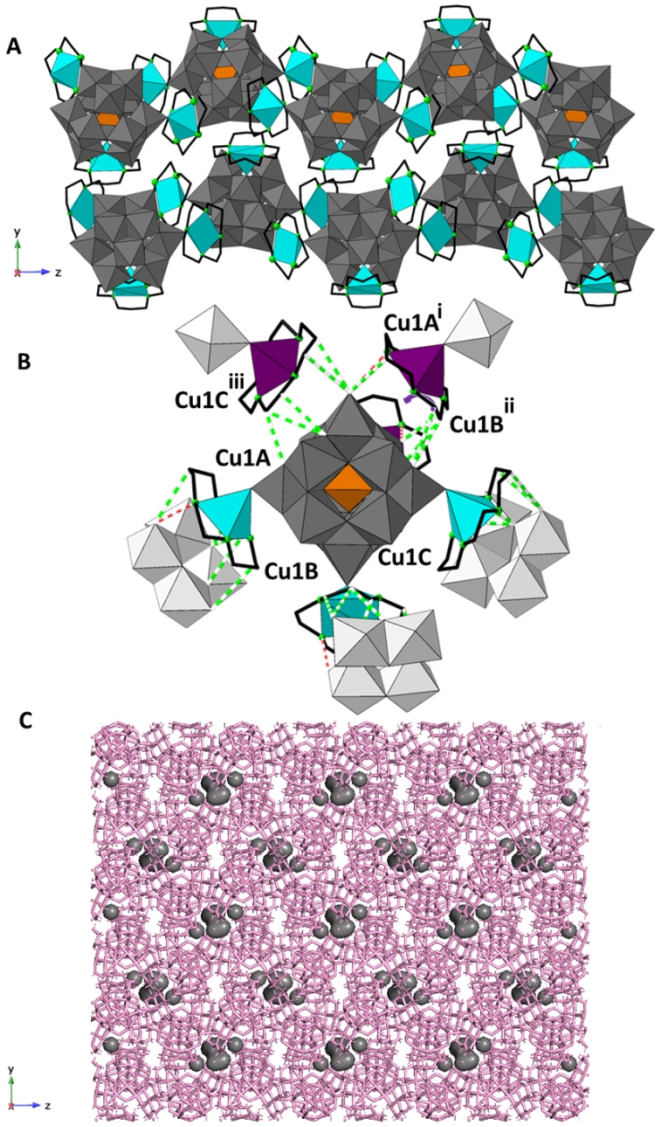

229x400mm (96 x 96 DPI)

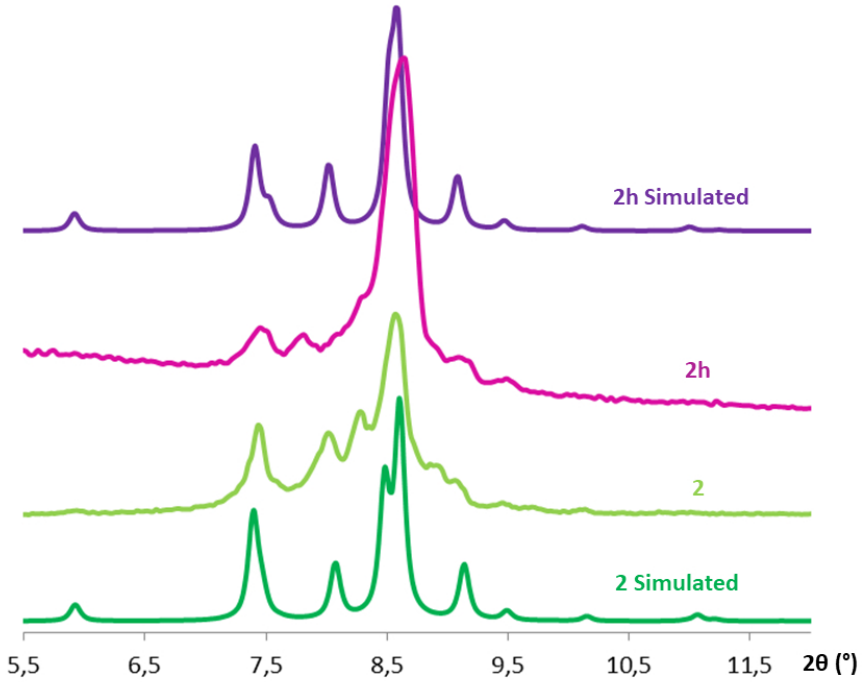

254x190mm (96 x 96 DPI)